Analytical Representation of Four-dimensional Hemodynamics for Drug Therapy Simulation in Acute Heart Failure Treatment

Yasuyuki Kataoka[1], Yukiko Fukuda[1], Jon Peterson[1], Shohei Yokota[2], Kazunori Uemura[2]
Keita Saku[2], Joe Alexander[1], Kenji Sunagawa[3]

Abstract—Acute heart failure imperils multiple organs, including the heart. Elucidating the impact of drug therapies across this multidimensional hemodynamic system remains a challenge. This paper proposes a simulator that analyzes the impact of drug therapies on four dimensions of hemodynamics: left atrial pressure, cardiac output, mean arterial pressure, and myocardial oxygen consumption. To mathematically formulate hemodynamics, the analytical solutions of four-dimensional hemodynamics and the direction of its change are derived as functions of cardiovascular parameters: systemic vascular resistance, cardiac contractility, heart rate, and stressed blood volume. Furthermore, a drug library which represents the multi-dependency effect of drug therapies on cardiovascular parameters was identified in animal experiments. In evaluating the accuracy of our derived hemodynamic direction, the average angular error of predicted versus observed direction was 18.85 [deg] after four different drug infusions for acute heart failure in animal experiments. Finally, the impact of drug therapies on four-dimensional hemodynamics was analyzed in three different simulation settings. One result showed that, even when drug therapies were simulated with simple rules according to the Forrester classification, the predicted direction of hemodynamic change matched the expected direction in more than 80% in 963 different AHF patient scenarios. Our developed simulator visualizes the impact of drug therapies on four-dimensional hemodynamics so intuitively that it can support clinicians' decision-making to protect multiple organs.

I. INTRODUCTION

In treating diverse scenarios of acute heart failure (AHF), predicting how drug therapies change hemodynamics is critical to support physicians' decisions [1]. For instance, inotropic agents can support and stabilize overall hemodynamics but they have not shown improved survival due to the increased myocardial oxygen (MVO_2) demand [2]. In AHF following coronary occlusion, managing MVO_2 is crucial to minimize infarction size and prevent myocardial remodeling [3], [4]. Thus, it is clinically useful to elucidate how drug therapies change multiple-dimensional hemodynamics including MVO_2.

To manage multiple hemodynamics, automated drug therapeutic systems that control up to three-dimensional hemodynamics were proposed via PID control [5]–[7]. To mathematically analyze hemodynamics, we proposed a drug infusion system with the analytical solutions of three-dimensional hemodynamics [8]. However, there remained challenges in
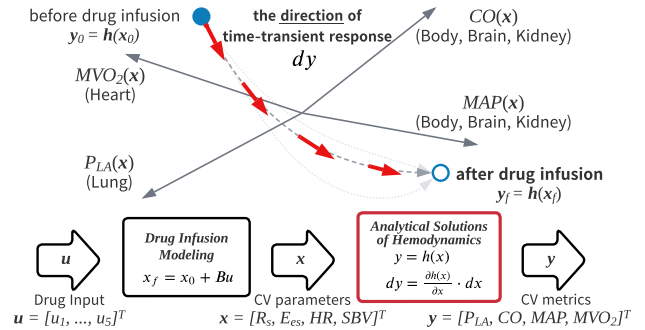
[1] NTT Research, Inc., Sunnyvale, CA 94085, USA, {yasuyuki.kataoka, yukiko.fukuda, jon.peterson, joe.alexander}@ntt-research.com
[2] National Cerebral and Cardiovascular Center, Suita, Osaka 564-8565, Japan, {yokota.shohei, kuemura, saku.keita}@ncvc.go.jp
[3] Circulatory System Research Foundation, Bunkyo-ku, Tokyo 113-0033, Japan, sunagawa.kenji.310@m.kyushu-u.ac.jp

Fig. 1: Hemodynamics analysis in drug therapies for AHF

elucidating hemodynamics such as analytical solutions of MVO_2, the time-transient response, and the pharmacokinetic modeling. This report presents a simulation system that can analyze the immediate directional change and the final outcome of four-dimensional hemodynamics after drug administration as shown in Fig.1.

The purpose of this paper is to derive and validate the direction of hemodynamic change caused by drug therapies, and to develop and evaluate a simulator that analyzes how drug therapies change four-dimensional hemodynamics.

In our methods, first, the multiple drug inputs u change the patient's cardiovascular parameters x (*CV parameters*): systemic vascular resistance (R_s [mmHg·sec/ml]), cardiac contractility (E_{es} [mmHg/ml]), heart rate (HR [beat/min]), and stressed blood volume (SBV [ml]). The key to model the relationship between u and x is to parametrize the multi-dependency effect from each drug input to each *CV parameters*. This paper identifies this relationship via an animal experiment in which four different drugs were administered. Second, *CV parameters* x change the patient's hemodynamics. In this paper, four-dimensional hemodynamics are defined as the patient's cardiovascular metrics y (*CV metrics*): left atrial pressure (P_{LA} [mmHg]), cardiac output (CO [L/min]), mean arterial pressure (MAP [mmHg]), and MVO_2 [ml O_2/min/100g]. In methods, it is shown that *CV metrics* y can be represented by a vector function of *CV parameters* x. Then, the direction of hemodynamic change dy is analytically derived by its total derivative. Integrating these technical contributions into a simulation tool, the outcomes of drug therapies to hemodynamics are visualized by 1) y_0 - the initial *CV metrics*, 2) dy - the immediate time-transient response of *CV metrics*, and 3) y_f - the final steady-state response *CV metrics* as shown in Fig.1.

In our experiments of drug therapies, the direction of

hemodynamic change was evaluated compared to the in-vivo response data. Moreover, the validity and value of our simulation tool are evaluated from a clinical perspective.

II. METHODS

Section II-A introduces the basics of our drug infusion system and three-dimensional hemodynamics analysis based on previous studies [8]. Thereafter, our new proposed methods are shown.

A. Fundamental basics from our past study

In the system representation, let $\boldsymbol{x}$ be the *CV parameters* $\boldsymbol{x} := [R_s, E_{es}, HR, SBV]^T \in \mathbb{R}^4$. Assuming $\boldsymbol{x}$ is measurable or possible to estimate, the patient's initial *CV parameters* $\boldsymbol{x}_0$ are given. Next, let the input $\boldsymbol{u}$ be the drug infusion $\boldsymbol{u} := [u_1, \cdots, u_5]^T \in \mathbb{R}^5$ which are key drugs used in treatment of AHF: Dobutamine (DOB) as a positive inotrope, Norepinephrine (NE) as a vasopressor, Sodium Nitroprusside (SNP) as a vasodilator, Dextran (DEX) as a fluid, and Furosemide (FRO) as a diuretic, respectively. Then, let $\boldsymbol{y}$ be the *CV metrics* $\boldsymbol{y} := [P_{LA}, CO, MAP, MVO_2]^T \in \mathbb{R}^4$. Remark MVO_2 is added from the past study [8].

First, drug infusion $\boldsymbol{u}$ directly affects *CV parameters* $\boldsymbol{x}$ based on their pharmacology. Thus, let *CV parameters* $\boldsymbol{x}$ be represented by a vector function $\boldsymbol{x} := \boldsymbol{f}(\boldsymbol{u}) \in \mathbb{R}^4$. The function $\boldsymbol{f}(\boldsymbol{u})$ in a steady state is modeled by

$$\boldsymbol{x}_f = \boldsymbol{B}\boldsymbol{u} + \boldsymbol{x}_0 \quad (1)$$

where $\boldsymbol{x}_0$ is the initial *CV parameters* and $\boldsymbol{x}_f$ is the final *CV parameters* following drug infusion. The input matrix $\boldsymbol{B}$ is the *drug library* that represents the multi-dependency effect from each drug to *CV parameters* in a steady state.

Changes in *CV parameters* $\boldsymbol{x}$ will in turn modulate *CV metrics* $\boldsymbol{y}$. In the previous study [8], the analytical solutions of $P_{LA}(\boldsymbol{x})$, $CO(\boldsymbol{x})$, $MAP(\boldsymbol{x})$ were derived from the intersection of the *Frank-Starling Curve* and *Guyton's Venous Return Curve* formula in [9] and [10] as

$$P_{LA}(\boldsymbol{x}) = -\alpha \left(\frac{aW\left(-\frac{b}{a}\exp\left(\frac{c}{a}\right)\right)}{b} \right) - \alpha \text{ [mmHg]} \quad (2)$$

$$CO(\boldsymbol{x}) = -aW\left(-\frac{b}{a}\exp\left(\frac{c}{a}\right)\right) + c \left[\frac{\text{L}}{\text{min}}\right] \quad (3)$$

$$MAP(\boldsymbol{x}) = \frac{1000}{60}CO(\boldsymbol{x})x_1 \text{ [mmHg]} \quad (4)$$

$$a = \frac{1}{1000}\frac{x_2 x_3}{\beta(x_2 + \frac{x_3}{60}x_1)} \quad (5)$$

$$b = -\frac{60}{1000}\frac{\alpha}{R_{vp}} \quad (6)$$

$$c = \frac{60}{1000}\frac{1}{R_{vp}}\left(\frac{x_4}{C_s + C_p} + \alpha\right) \quad (7)$$

where $W(\cdot)$ is defined as the Lambert function, where α and β are the end-diastolic pressure-volume relationship (ED-PVR) parameters, and where R_{vp}, C_p, C_s are the resistance for pulmonary venous return, the compliance in the pulmonary circulation and the systemic circulation, respectively.

TABLE I: Constant Parameters of MVO_2 model

Param.	Value	Unit
A_o	1.8×10^{-5}	[ml O$_2$/mmHg/ml]
B_o	2.4×10^{-3}	[ml O$_2$·ml/mmHg/beat/100g]
C_o	1.4×10^{-2}	[ml O$_2$/beat/100g]

B. Analytical Solution of Myocardial Oxygen Consumption

Metabolic demand of the heart itself is a key indicator to prevent poor prognosis, re-hospitalization, adverse cardiovascular events, or mortality in AHF treatment.

Based on the mechanical energy generated by ventricular contraction, myocardial oxygen consumption of the left ventricle, MVO_2 [ml O$_2$/min/100g], can be represented as a function of *CV parameters* $\boldsymbol{x}$ by

$$MVO_2(\boldsymbol{x}) = (A_o PVA(\boldsymbol{x}) + B_o x_2 + C_o)x_3 \quad (8)$$

where A_o, B_o, and C_o are the constant parameters shown in TABLE I and $PVA(\boldsymbol{x})$ [mmHg·ml/100g/beat] is the normalized pressure volume area per 100 [g] of the left ventricle [11]. Assuming the weight of left ventricle is 0.4% of the total body weight (BW [kg]) [12], the normalized $PVA(\boldsymbol{x})$ can be represented as a function of *CV parameters* $\boldsymbol{x}$ by

$$PVA(\boldsymbol{x}) = \left(\frac{MAP(\boldsymbol{x})^2}{2x_2} + \frac{CO(\boldsymbol{x})MAP(\boldsymbol{x})}{x_3} \right) \frac{25}{BW}. \quad (9)$$

Thus, MVO_2 can also be represented as a function of $\boldsymbol{x}$.

C. Direction of hemodynamic change

The analytical solution of the direction of hemodynamic change can quantify the effect of how slight *CV parameters* change $d\boldsymbol{x}$ contributes to the slight *CV metrics* change $d\boldsymbol{y}$.

Let *CV metrics* $\boldsymbol{y}$ be represented by a vector function $\boldsymbol{h}(\boldsymbol{x}) := [P_{LA}(\boldsymbol{x}), CO(\boldsymbol{x}), MAP(\boldsymbol{x}), MVO_2(\boldsymbol{x})]^T \in \mathbb{R}^4$. The direction of hemodynamic change can be derived by the total derivative of $\boldsymbol{y}$,

$$d\boldsymbol{y} = \frac{\partial \boldsymbol{h}(\boldsymbol{x})}{\partial \boldsymbol{x}} d\boldsymbol{x} = \begin{bmatrix} \langle \nabla CO(\boldsymbol{x}), d\boldsymbol{x} \rangle \\ \langle \nabla P_{LA}(\boldsymbol{x}), d\boldsymbol{x} \rangle \\ \langle \nabla MAP(\boldsymbol{x}), d\boldsymbol{x} \rangle \\ \langle \nabla MVO_2(\boldsymbol{x}), d\boldsymbol{x} \rangle \end{bmatrix} \quad (10)$$

$$\frac{\partial \boldsymbol{h}(\boldsymbol{x})}{\partial \boldsymbol{x}} = \begin{bmatrix} \frac{\partial CO(\boldsymbol{x})}{\partial R_s} & \frac{\partial CO(\boldsymbol{x})}{\partial E_{es}} & \frac{\partial CO(\boldsymbol{x})}{\partial HR} & \frac{\partial CO(\boldsymbol{x})}{\partial SBV} \\ \frac{\partial P_{LA}(\boldsymbol{x})}{\partial R_s} & \frac{\partial P_{LA}(\boldsymbol{x})}{\partial E_{es}} & \frac{\partial P_{LA}(\boldsymbol{x})}{\partial HR} & \frac{\partial P_{LA}(\boldsymbol{x})}{\partial SBV} \\ \frac{\partial MAP(\boldsymbol{x})}{\partial R_s} & \frac{\partial MAP(\boldsymbol{x})}{\partial E_{es}} & \frac{\partial MAP(\boldsymbol{x})}{\partial HR} & \frac{\partial MAP(\boldsymbol{x})}{\partial SBV} \\ \frac{\partial MVO_2(\boldsymbol{x})}{\partial R_s} & \frac{\partial MVO_2(\boldsymbol{x})}{\partial E_{es}} & \frac{\partial MVO_2(\boldsymbol{x})}{\partial HR} & \frac{\partial MVO_2(\boldsymbol{x})}{\partial SBV} \end{bmatrix} \quad (11)$$

$$d\boldsymbol{x} = \begin{bmatrix} dR_s, dE_{es}, dHR, dSBV \end{bmatrix}^T. \quad (12)$$

The columns of *Jacobian* (11) shows the sensitivity of how the change of single *CV parameter* x_i affects multiple *CV metrics* $\boldsymbol{y}$. The row of *Jacobian* (11), which is also expressed by $\nabla h_i(\boldsymbol{x}) = [\frac{\partial h_i(\boldsymbol{x})}{\partial R_s}, \frac{\partial h_i(\boldsymbol{x})}{\partial E_{es}}, \frac{\partial h_i(\boldsymbol{x})}{\partial HR}, \frac{\partial h_i(\boldsymbol{x})}{\partial SBV}]$, shows the sensitivity of how the change of multiple *CV parameters* $\boldsymbol{x}$ affects single *CV metric* y_i. The *Jacobian* (11) can be analytically solved using the derivative of Lambert function,

$$\frac{dW(z)}{dz} = \frac{1}{z + e^{W(z)}} \left(z \neq -\frac{1}{e} \right). \quad (13)$$

D. Drug Library Development via Animal Experiment

The change of *CV parameters* $\boldsymbol{x}$ from initial to final values is determined by $\boldsymbol{Bu}$ in (1). The key parameter, the drug library $\boldsymbol{B}$, was identified in the following method.

1) Animal Experiment Protocol: In preparation, a dog was anesthetized and the bilateral carotid baroreceptors and vagal trunk were denervated. After thoracotomy, the animal was connected to a system that measures MAP from the right femoral artery, CO via ultrasonic flow meter around the ascending aorta, both P_{LA} and P_{RA} (right atrial pressure) directly in atria, and HR.

Prior to drug infusion, the baseline was measured for 1 minute. Next, a single drug was administered for 10 minutes to measure pharmacological effect until steady state. Then, minimal washout time was ensured until MAP stabilized at the pre-drug value. The same procedures were repeated for the other drugs. In this experiment, DOB = 5.0 [μg/kg/min], NE = 0.15 [μg/kg/min], SNP = 5.0 [μg/kg/min], and DEX = 5.0 [ml/kg] were infused.

This protocol was approved by the animal subjects committee of the *National Cerebral and Cardiovascular Center.*

2) Drug Library Identification: To develop the drug library $\boldsymbol{B}$, the gains from each drug input u_i to each *CV parameters* x_i change were identified by fitting to the 1st order single-input single-output process model with dead time, where R_s is computed by $60(MAP - P_{RA})/CO$, where E_{es} is estimated by our estimation method[1] based on the cardiac mechanics, where HR is measurable from a sensor, and where SBV is *stressed blood volume* estimated by the circulatory equilibrium framework [13].

Aggregating the identified gains, the drug library $\boldsymbol{B}$ became

$$\boldsymbol{B} = \begin{bmatrix} -0.0335 & 3.33 & -0.419 & -0.00725 & 0 \\ 3.88 & 26.1 & -1.14 & -0.0135 & 0 \\ 8.10 & 24.9 & 0.164 & -0.450 & 0 \\ 27.7 & 76.2 & -14.1 & 1.47 & -c \cdot BW \end{bmatrix}. \quad (14)$$

Note that FRO was not identified based on real data for this protocol. Here, it is assumed to simply decrease only SBV.

III. Results

A. Exp.1 Derived Direction Comparison to Real Response

The purpose of *Exp.1* is to validate the direction of hemodynamic change shown in (10). Our proposed direction is compared to the real direction of hemodynamic change after four different drug infusions in animal experiments. The performance is evaluated in (P_{LA}, CI) space because this is a common metrics space known as *Forrester classification* in AHF treatment, where CI is *cardiac index* defined by CO/BSA (body surface area).

[1]The details are provided in another paper accepted for the same conference: "Inverse ESPVR Estimation with Singularity Avoidance via Constrained EDPVR Parameter Optimization."

TABLE II: Constant Parameters used in Experiments

Const.	Value	Unit ($\gamma = \mu$g/kg/min)	Description
α	0.86	unitless	EDPVR
β	0.15	unitless	EDPVR
C_p	3.0	[ml/mmHg]	Pulmonary Compliance
C_s	17	[ml/mmHg]	Systemic Compliance
R_{vp}	0.25	[mmHg·sec/ml]	Pulmonary VR Resistance
BW	9.7	[kg]	Body Weight
BSA	0.47	[m^2]	Body Surface Area
c	20	[ml/mg]	Gain param. FRO $\rightarrow SBV$

1) Setting of Exp.1: The real responses from the animal experiment after drug infusion are denoted by P_{LA_r} and CI_r. To evaluate the direction angle, P_{LA_r} and CI_r need to be normalized because they have different dimensions and data ranges. Given the time step k that increments every 30 [sec] and the measured *CV parameters* $\boldsymbol{x}[k]$, let the normalized vector of real response at the time of k be

$$\boldsymbol{dy}_r[k] = \left(\frac{P_{LA\_r}[k+1] - P_{LA\_r}[k]}{\overline{P_{LA\_r}}}, \frac{CI_r[k+1] - CI_r[k]}{\overline{CI_r}} \right) \quad (15)$$

where $\overline{P_{LA\_r}}$ and $\overline{CI_r}$ are the peak-to-peak values in each dimension.

The proposed directions of hemodynamic change are considered in two different versions. The first version is the original total derivative that uses the one-step future *CV parameters* $\boldsymbol{x}[k+1]$,

$$\boldsymbol{dy}_f[k] = (dP_{LA\_f}[k], dCI_f[k]) \quad (16)$$

$$dP_{LA\_f}[k] = \frac{\langle \nabla P_{LA}(\boldsymbol{x}[k]), \boldsymbol{x}[k+1] - \boldsymbol{x}[k] \rangle}{\overline{P_{LA\_r}}} \quad (17)$$

$$dCI_f[k] = \frac{\langle \nabla CI(\boldsymbol{x}[k]), \boldsymbol{x}[k+1] - \boldsymbol{x}[k] \rangle}{\overline{CI_r}}. \quad (18)$$

The second version is the approximated total derivative that uses the one-step past *CV parameters* $\boldsymbol{x}[k-1]$,

$$\boldsymbol{dy}_p[k] = (dP_{LA\_p}[k], dCI_p[k]) \quad (19)$$

$$dP_{LA\_p}[k] = \frac{\langle \nabla P_{LA}(\boldsymbol{x}[k]), \boldsymbol{x}[k] - \boldsymbol{x}[k-1] \rangle}{\overline{P_{LA\_r}}} \quad (20)$$

$$dCI_p[k] = \frac{\langle \nabla CI(\boldsymbol{x}[k]), \boldsymbol{x}[k] - \boldsymbol{x}[k-1] \rangle}{\overline{CI_r}}. \quad (21)$$

While $\boldsymbol{dy}_f[k]$ is expected to be more accurate, $\boldsymbol{dy}_p[k]$ is more practical for the application that predicts the direction based on only the past information. The constant parameters are shown in TABLE II, which were tuned by the body weight.

The evaluation metrics for the directional difference are

$$i) \ Error \ \theta_{rf} = \arccos \left(\frac{\langle \boldsymbol{dy}_r[k], \boldsymbol{dy}_f[k] \rangle}{|\boldsymbol{dy}_r[k]||\boldsymbol{dy}_f[k]|} \right) \quad (22)$$

$$ii) \ Error \ \theta_{rp} = \arccos \left(\frac{\langle \boldsymbol{dy}_r[k], \boldsymbol{dy}_p[k] \rangle}{|\boldsymbol{dy}_r[k]||\boldsymbol{dy}_p[k]|} \right) \quad (23)$$

where $\theta_{rf}[k]$ is the error angle between $\boldsymbol{dy}_r[k]$ and $\boldsymbol{dy}_f[k]$, and $\theta_{rp}[k]$ is the error angle between $\boldsymbol{dy}_r[k]$ and $\boldsymbol{dy}_p[k]$.
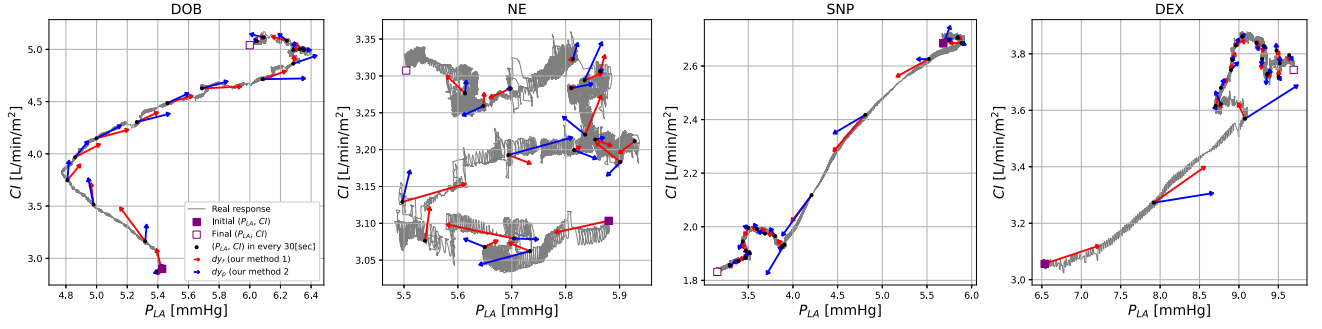
Fig. 2: The proposed directions of hemodynamic change compared to real response (gray: dy_r, red: dy_f, blue: dy_p)

TABLE III: Results of Exp.1 - Angular Errors (Real vs Ours)

Drug	i) Error θ_{rf}		ii) Error θ_{rp}	
	Error avg. [°]	C.I. [°]	Error avg. [°]	C.I. [°]
DOB	16.1	[10.4, 21.9]	38.0	[19.7, 56.4]
NE	28.1	[9.7, 46.4]	57.2	[30.7, 83.8]
SNP	14.0	[9.1, 18.9]	39.3	[22.5, 56.1]
DEX	17.2	[10.8, 23.7]	47.6	[27.3, 68.0]

2) Results of Exp.1: Fig. 2 visualizes the results of the real drug response and our proposed directions of hemodynamic change at every 30 [sec]. Visually, both versions of our methods, $dy_f[k]$ and $dy_p[k]$, accurately predict the direction at each time step k.

TABLE. III shows the results of the angular error compared to the real response and our proposed directional changes via total derivatives by its average value and confidence interval (C.I.). On the average of the 4 drug infusion experiments, $Error\ \theta_{rf}$ resulted in 18.85 [°]. In the practical prediction task when the future information is not available, the average $Error\ \theta_{rp}$ resulted in 45.5 [°].

B. Exp.2 Analysis on impacts of drug inputs to CV metrics

The purpose of *Exp.2* is to evaluate our developed simulator that analyzes how drug therapies change four-dimensional hemodynamics. Our developed system integrated i) the drug infusion model $x = f(u)$ in (1) with the identified drug library B in (14), and ii) the hemodynamics analytical solutions $y = h(x) = h(f(u))$ and the direction of its change dy in (10). Then, three simulation studies were conducted to evaluate our system in both qualitative and quantitative manner: 1) single drug infusion, 2) three AHF scenarios, 3) recommended drug therpies via *Forrester classification*.

1) Single Drug Infusion:

a) Setting - This simulation experiment visualizes how single drug infusion u_i affects four-dimensional hemodynamics y with the direction of its change. The infused single dose is set as $u_1 = 2.0$ [μg/kg/min] for DOB, $u_2 = 0.15$ [μg/kg/min] for NE, $u_3 = 2.0$ [μg/kg/min] for SNP, $u_4 = 75$ [ml] for DEX, and $u_5 = 5.0$ [mg] for FRO. For the simulated AHF patients, the different combinations of *CV parameters* were formed by $R_s = [1.0, 3.0, 5.0]$, $E_{es} = [6.0, 12.0]$, $HR = [60, 120]$, and $SBV = [100 : 150 : 700]$.

b) Results - The simulation results are shown in Fig. 3. For better visualization, the *CV metrics* are divided into two spaces: 1) $LAP - CI$ (*Forrester classification*) and
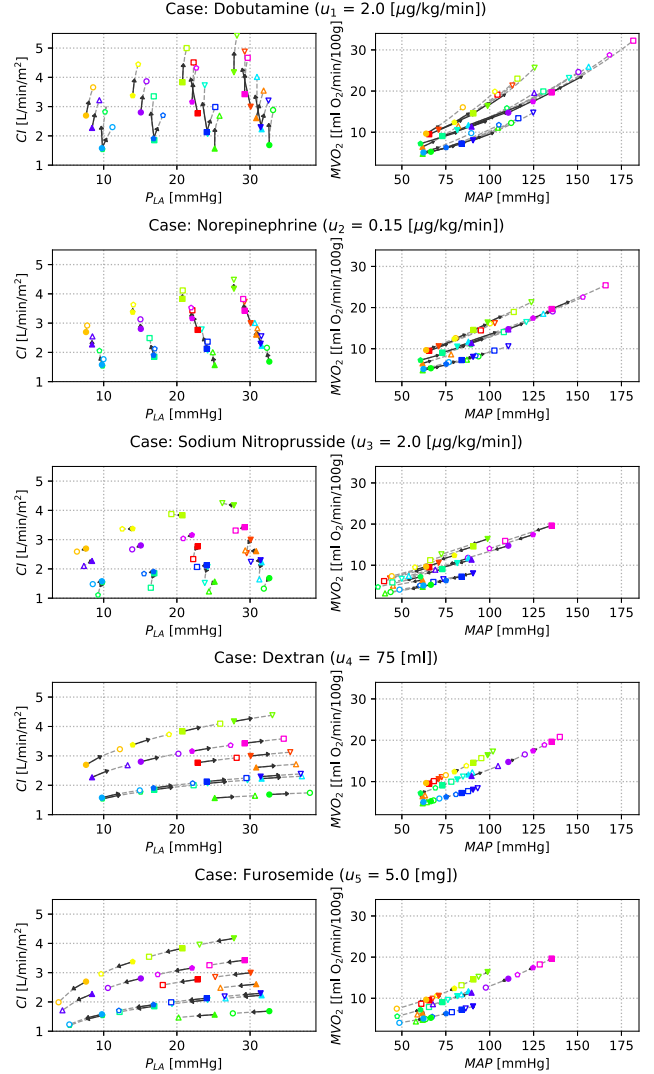

Fig. 3: Results of single drug infusion: Each filled marker shows the initial *CV metrics* y_0 of different AHF patients. The black arrow shows the direction of hemodynamic change dy. The gray dashed line implies the estimated time-transient response using Bezier curve. Each empty marker shows the final outcome in steady-state y_f.

2) $MAP - MVO_2$. These results indicated that positive inotropes (DOB, NE) improve CI and MAP but significantly increase MVO_2, while SNP and FRO decrease LAP
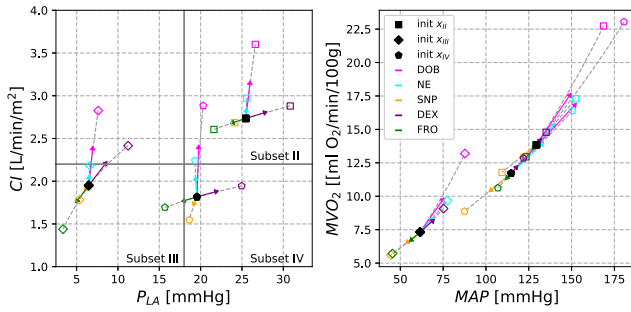
Fig. 4: Results of the three AHF scenarios ($\boldsymbol{x}_{II}, \boldsymbol{x}_{III}, \boldsymbol{x}_{IV}$)

and MVO_2. This visualization provides meaningful insight for physicians because LAP and MAP are measurable in clinical practice, but MVO_2 is not directly measurable.

2) Three AHF Scenarios:

a) Setting - This simulation visualizes three specific clinical scenarios in Subset II, III, and IV on *Forrester classification*. Three representative patients with the following *CV parameters* were considered.

- (warm & wet) $\boldsymbol{x}_{II} = [6.0, 15, 80, 600]^T$
- (cold & dry) $\boldsymbol{x}_{III} = [4.0, 10, 100, 200]^T$
- (cold & wet) $\boldsymbol{x}_{IV} = [8.0, 8.0, 100, 450]^T$

Then, each drug infusion was simulated. The dosage was set to be the same amount mentioned in the section III-B.1

b) Results - The single-drug infusion impacts on each clinical scenario are shown in Fig. 4. The initial direction and the time-transient response correspond to the expectation of pharmacological effects in general. It was also visualized that even with the same drug and the same dose, there are differences in sensitivity depending on the patient's condition. For example, the DOB administration ($2.0\,[\mu\mathrm{g/kg/min}]$) improves CI in all scenarios, and the change of MVO_2 in Subset IV is notably more significant than in other scenarios:

- (warm & wet) $\boldsymbol{x}_{II}$: +8.88 [ml O$_2$/min/100g]
- (cold & dry) $\boldsymbol{x}_{III}$: +5.87 [ml O$_2$/min/100g]
- (cold & wet) $\boldsymbol{x}_{IV}$: +11.3 [ml O$_2$/min/100g].

The mechanism of such a nonlinear behavior is caused by the gradients of $MVO_2(\boldsymbol{x})$ derived in (11). This means that the same dosage of DOB results in greater oxygen consumption in the heart for patients in Subset IV than for other patients.

3) Recommended drug therapies via Forrester classification:

a) Setting - This simulation validates whether our predicted direction of hemodynamic change is oriented towards the desired range in (P_{LA}, CI) space when the recommended drug therapies are applied for various AHF patients. For the simulated AHF patients, the different combinations of *CV parameters* were formed by $R_s = [1.0 : 1.0 : 5.0]$, $E_{es} = [3.0 : 2.0 : 15.0]$, $HR = [60 : 20 : 150]$, and $SBV = [100 : 50 : 700]$. Then, the unrealistic AHF patients with $MAP(\boldsymbol{x}) \leq 45\,[\mathrm{mmHg}]$ or $170\,[\mathrm{mmHg}] \leq MAP(\boldsymbol{x})$ were excluded. As a result, 963 different AHF patients were simulated.

To treat these AHF patients, the drug combinations and the dosages were selected based on the guideline in the *Forrester classification*.
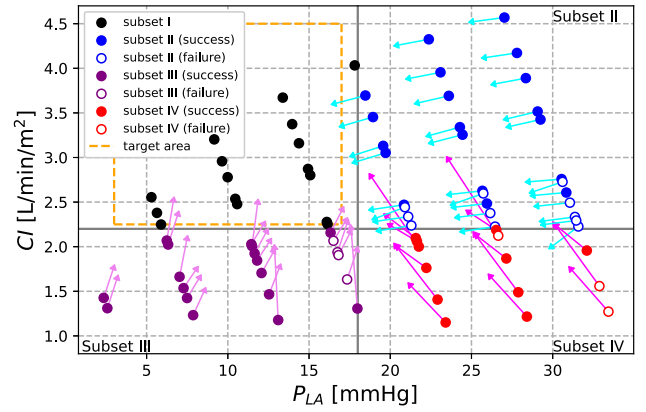

Fig. 5: Results of recommended drug therapies by *Forrester classification* ($\boldsymbol{u}_{II}, \boldsymbol{u}_{III}, \boldsymbol{u}_{IV}$)

- Subset II : $\boldsymbol{u}_{II}$ = $[0.0, 0.0, 5.0, 0.0, 1.5]^T$
- Subset III : $\boldsymbol{u}_{III}$ = $[5.0, 0.15, 0.0, 50.0, 0]^T$
- Subset IV : $\boldsymbol{u}_{IV}$ = $[5.0, 0.0, 5.0, 0.0, 1.5]^T$

The evaluation metrics is whether the extension of the predicted direction from the initial state belongs to the target area that is set within the Subset I: $3.0 \leq P_{LA} \leq 17.0\,[\mathrm{mmHg}]$ and $2.25 \leq CI \leq 4.5\,[\mathrm{L/min/m^2}]$.

b) Results - As a result of evaluating the directions of hemodynamic change, 779 AHF patients out of 963 patients were successfully oriented towards the target area (80.9%), even though the drug inputs are simply fixed for each subset. Fig. 5 shows the simulation result of *Exp.2* with the thinned-out parameters for better visualization. These results of directional orientation mostly correspond to the expected results in the clinical guideline. Thus, our overall system, including the identified drug library $\boldsymbol{B}$ and the analytical solutions, is reasonably correct.

IV. DISCUSSION

A. Clinical values of the proposed simulator

This study allows us to simultaneously visualize how each drug affects cardiac metabolism (MVO_2) as well as the circulatory system (CI, MAP, LAP). For example, positive inotropes (such as catecholamines) are crucial for maintaining adequate hemodynamic stability and preventing hypoperfusion or pulmonary congestion. Conversely, an increase in their usage can result in a poorer prognosis for patients with cardiogenic shock since the utilization of these drugs can lead to metabolic stress and arrhythmogenesis in a depressed heart [14]. Thus, it is very difficult to determine which dosage of the drug is appropriate in clinical practice [15].

As in the various examples shown in this paper such as Fig. 3 or Fig. 4, our proposed drug therapy analysis tool will assist physicians in making decisions regarding treatment by visualizing how drugs act on the whole body as well as the heart. It is also clearly revealed that the sensitivity varies depending on the patient's *CV parameters* or AHF scenario, even if the dose is the same. Our new method of gradient analysis allows us to analytically quantify the

immediate change of drug therapies instantly, providing realtime decision support.

Our proposed system can be applied to analyze the effects of other drugs that were not considered in this paper. For example, the use of beta-blockers should be considered because early administration of beta-blockers has been reported to improve prognosis and to prevent sudden death resulting from arrhythmias [2]. Additionally, the use of a pure bradycardic agent (Ivabradine) with conventional drugs is reported to improve the performance of simultaneous four-dimensional hemodynamics control in dogs with acute heart failure [16]. Beyond the analysis of single drug administration, our systematic approach can simulate the combination of multiple drug administrations as in Fig. 5, which supports physicians in developing an optimal treatment strategy.

B. Limitation and Future Study

As shown in Fig. 1, while our proposed method indicates the direction of hemodynamic change when *CV parameters* is measured at each time, the present system does not predict the entire time-transient response. If the pharmacokinetics is modeled accurately, the time function of *CV parameters* $x(t)$ would help to describe the overall time-transient response.

The identified drug library depends on data from a single animal experiment. More animal experiments are required to statistically verify these results.

The analytical solution assumes that total volume is distributed by the compliance ratio of systemic and pulmonary circulation. To identify the proportion accurately, the functional balance between the left and right ventricles needs to be considered.

In the human cardiovascular system, multiple regulatory systems stabilize hemodynamics such as the baroreflex system. Also, the changes in coronary arterial pressure affect the end-systolic pressure-volume relationship [17], which is a feedback biomechanism $y_3 \rightarrow x_2$. Our system needs to explicitly consider them.

Based on these analytical studies and simulators, we aim to construct a closed-loop autonomous treatment system whose control stability is analytically guaranteed.

V. Conclusion

In this paper, the mechanism of pharmacological effects on hemodynamics was mathematically analyzed and clinically discussed for its clinical usefulness. One notable technical contribution is the derived analytical solution for the direction of hemodynamic change after drug administration. In addition, the effects of drug inputs on cardiovascular parameters were identified with real data obtained in animal experiments. With a system that combines these results, it became possible to analyze the impact of pharmacological effects on four-dimensional hemodynamics for various AHF scenarios. This system would support clinical treatment decisions that protect multiple organs in AHF treatment especially by foreseeing myocardial oxygen consumption. In the future, we will conduct more animal experiments to verify the validity of these methods and explore more clinically useful applications.

References

[1] T. M. Maddox, J. L. Januzzi, L. A. Allen, K. Breathett, J. Butler, L. L. Davis, and et al., "2021 Update to the 2017 ACC Expert Consensus Decision Pathway for Optimization of Heart Failure Treatment: Answers to 10 Pivotal Issues About Heart Failure With Reduced Ejection Fraction: A Report of the American College of Cardiology Solution Set Oversight Committee," *Journal of the American College of Cardiology*, vol. 77, no. 6, pp. 772–810, 2021.

[2] P. A. Heidenreich, B. Bozkurt, D. Aguilar, L. A. Allen, J. J. Byun, M. M. Colvin, and et al., "2022 AHA/ACC/HFSA Guideline for the Management of Heart Failure A Report of the American College of Cardiology/American Heart Association Joint Committee on Clinical Practice Guidelines," *Journal of the American College of Cardiology*, vol. 79, no. J Am Coll Cardiol 63 2014, pp. e263–e421, 2022.

[3] K. D. Müller, S. Sass, M. G. Gottwik, and W. Schaper, "Effect of myocardial oxygen consumption on infarct size in experimental coronary artery occlusion," *Basic Research in Cardiology*, vol. 77, no. 2, pp. 170–181, 1982.

[4] N. Uriel, G. Sayer, S. Annamalai, N. K. Kapur, and D. Burkhoff, "Mechanical Unloading in Heart Failure," *Journal of the American College of Cardiology*, vol. 72, no. 5, pp. 569–580, 2018.

[5] T. Nishikawa, K. Uemura, Y. Hayama, T. Kawada, K. Saku, and M. Sugimachi, "Development of an automated closed-loop β-blocker delivery system to stably reduce myocardial oxygen consumption without inducing circulatory collapse in a canine heart failure model: a proof of concept study," *Journal of Clinical Monitoring and Computing*, vol. 36, no. 3, pp. 849–860, 2022.

[6] K. Uemura, M. Sugimachi, T. Kawada, and K. Sunagawa, "Automated drug delivery system for the management of hemodynamics and cardiac energetic in acute heart failure," *32nd Annual International Conference of the IEEE EMBSB*, vol. 2010, pp. 5222–5, 2010.

[7] K. Kashihara, "Automatic Regulation of Hemodynamic Variables in Acute Heart Failure by a Multiple Adaptive Predictive Controller Based on Neural Networks," *Annals of Biomedical Engineering*, vol. 34, no. 12, pp. 1846–1869, 2006.

[8] Y. Kataoka, Y. Fukuda, J. Peterson, I. Shelly, J. Alexander, and K. Sunagawa, "System Design for Optimizing Drug Infusions Using Cardiovascular Space Mapping for Acute Heart Failure," *2022 44th Annual International Conference of the IEEE Engineering in Medicine & Biology Society (EMBC)*, pp. 1388–1393, 2022.

[9] K. Sunagawa, W. L. Maughan, D. Burkhoff, and K. Sagawa, "Left ventricular interaction with arterial load studied in isolated canine ventricle," *American Physiological Society*, vol. 245, no. 5 Pt 1, pp. H773–80, 1983.

[10] A. C. Guyton, A. W. Lindsey, B. Abernathy, and T. Richardson, "Venous Return at Various Right Atrial Pressures and the Normal Venous Return Curve," *American Journal of Physiology-Legacy Content*, vol. 189, no. 3, pp. 609–615, 1957.

[11] H. Suga, Y. Yasumura, T. Nozawa, S. Futaki, Y. Igarashi, and Y. Goto, "Prospective prediction of O2 consumption from pressure-volume area in dog hearts," *American Journal of Physiology-Heart and Circulatory Physiology*, vol. 252, no. 6, pp. 1258–1264, 1987.

[12] A. R. Casha, L. Camilleri, A. Manché, R. Gatt, M. Gauci, M.-T. Camilleri-Podesta, J. N. Grima, M. Scarci, and S. Chetcuti, "Physiological rules for the heart, lungs and other pressure-based organs," *Journal of Thoracic Disease*, vol. 9, no. 10, pp. 3793–3801, 2017.

[13] K. Uemura, T. Kawada, A. Kamiya, T. Aiba, I. Hidaka, K. Sunagawa, and M. Sugimachi, "Prediction of circulatory equilibrium in response to changes in stressed blood volume," *American Journal of Physiology-Heart and Circulatory Physiology*, vol. 289, no. 1, pp. 301–307, 2005.

[14] W. O'Neill, "Update from the national cardiogenic shock initiative," *Interventional Cardiology Review*, vol. 14, pp. 19–20, 2019.

[15] K. Ameloot, P. Jakkula, J. Hästbacka, M. Reinikainen, V. Pettilä, and et al., "Optimum Blood Pressure in Patients With Shock After Acute Myocardial Infarction and Cardiac Arrest," *Journal of the American College of Cardiology*, vol. 76, no. 7, pp. 812–824, 2020.

[16] K. Uemura, K. Sunagawa, and M. Sugimachi, "Computationally Managed Bradycardia Improved Cardiac Energetics While Restoring Normal Hemodynamics in Heart Failure," *Annals of Biomedical Engineering*, vol. 37, no. 1, pp. 82–93, 2009.

[17] K. Sunagawa, W. L. Maughan, G. Friesinger, P. Guzman, M. S. Chang, and K. Sagawa, "Effects of coronary arterial pressure on left ventricular end-systolic pressure-volume relation of isolated canine heart." *Circulation Research*, vol. 50, no. 5, pp. 727–734, 1982.